Available online at www.sciencedirect.com
ScienceDirect
Vision Research 47 (2007) 1935–1949
Vision Research
www.elsevier.com/locate/visres

Chromatic tuning of contour-shape mechanisms revealed through the shape-frequency and shape-amplitude after-effects

Elena Gheorghiu *, Frederick A.A. Kingdom

McGill Vision Research, Department of Ophthalmology, McGill University, 687 Pine Avenue W., Montreal H3A 1A1, Que., Canada

Received 12 December 2006; received in revised form 8 February 2007

Abstract

We investigated whether contour-shape processing mechanisms are selective for color direction using the shape-frequency and shape-amplitude after-effects, or SFAE and SAAE [Gheorghiu, E. & Kingdom, F. A. A. (2006). Luminance-contrast properties of contour-shape processing revealed through the shape-frequency after-effect. *Vision Research, 46*(21), 3603–3615. Gheorghiu, E. & Kingdom, F. A. A. (2007). The spatial feature underlying the shape-frequency and shape-amplitude after-effects. *Vision Research, 47*(6), 834–844]. All contours were defined along the 'red-green', 'blue-yellow' and 'luminance' axes of cardinal color space. Adapting and test contours were defined along the same or along opposite polarities within a cardinal axis, and along the same or along different cardinal axes. We found (i) little transfer of the after-effects across different within-axis polarities, for all cardinal axes and for both even-symmetric and odd-symmetric contours; (ii) little transfer between the red–green and blue–yellow cardinal axes; (iii) little transfer between the chromatic and luminance cardinal directions for the SAAE; (iv) large transfer between the chromatic and luminance cardinal directions for the SFAE. We conclude that contour-shape mechanisms are selective for within-cardinal axis polarity and for the chromatic axes within the isoluminant plane. However for certain types of contour-shape processing they are poorly selective along the chromatic versus luminance dimension. Overall our results suggest that contour-shape encoding mechanisms are selective for color direction and that color is important for contour-shape processing.

Keywords: Color; Contrast-polarity; Shape; Adaptation; Shape-frequency after-effect; Shape-amplitude after-effect

1. Introduction

Natural contours, such as edges and lines, typically vary along multiple photometric dimensions such as contrast, luminance phase, blur and chromaticity. Models of early human vision concerned with contour processing invariably use operators that are selective to these dimensions; for example linear filters such as simple cells tuned to different scales and orientations. An important question is which characteristics of a contour's luminance and chromatic profile are preserved for higher visual functions such as shape processing. Gheorghiu and Kingdom (2006) have suggested that there are broadly speaking two classes of early vision model that deal with this issue. They differ in the way information from different scale filters and from the positive and negative parts of filter outputs are combined to produce a feature description of the image. One class of model, which we have termed 'feature-rich', explicitly represents characteristics such as phase, scale and polarity at higher stages. Examples are Marr's (1982) and Marr and Hildreth's (1980) model of the primal sketch, Watt's (1988) and Watt and Morgan's (1985) MIRAGE model, Hesse and Georgeson's (2005) model of feature localization. The other class of model, which we have termed 'feature-agnostic', does not represent such characteristics at higher stages. Moronne and Burr's (1988) local energy model would seem to be an example of this class of model as it delivers a phaseless map of the locations of local energy peaks to higher stages of processing.

* Corresponding author.
E-mail address: elena.gheorghiu@mcgill.ca (E. Gheorghiu).

0042-6989/$ - see front matter © 2007 Elsevier Ltd. All rights reserved.
doi:10.1016/j.visres.2007.03.010

In this communication we consider whether contour-shape encoding mechanisms are selective for color direction, and hence whether feature-rich or feature-agnostic. By color direction we mean the angle of a vector in a three-dimensional color space that includes an isoluminant (chromatic-only) color plane and a luminance axis. We are not primarily concerned here with whether or not contour-shape mechanisms are sensitive to isoluminant stimuli, that is responsive or not to a stimulus defined solely by chromatic contrast, as considered by Mullen and Beaudot (2002). Our aim instead is to determine whether contour-shape encoding mechanisms are *selective to color direction*, that is tuned to particular colors or ranges of colors. We ask whether color direction can be added to luminance blur and luminance phase as photometric dimensions to which contour-shape mechanisms are selective (Gheorghiu & Kingdom, 2006). We are not aware of any previous studies that have investigated the chromatic selectivity of shape processing.

To explore the selectivity of contour-shape mechanisms to color direction, we have employed two recently discovered contour-shape after-effects: the shape-frequency and shape-amplitude after-effects, or SFAE and SAAE (Gheorghiu & Kingdom, 2006, 2007; Kingdom & Prins, 2005a, 2005b). The SFAE and SAAE are the perceived shifts in, respectively, the shape-frequency and shape-amplitude of a sinusoidal test contour following adaptation to a sinusoidal contour of slightly different shape-frequency/amplitude. As with other spatial after-effects such as the tilt and luminance-spatial-frequency after-effects, the perceived shifts in the SFAE and SAAE are always in a direction away from that of the adaptation stimulus. Readers can experience the SFAE and the SAAE in Fig. 1a and b by first moving their eyes back and forth along the horizontal markers on the left for about a minute, and then transferring their gaze to the central spot on the right. The two test contours, which are identical, should appear different in shape-frequency or shape-amplitude. An important property of both after-effects is that they survive shape-phase randomization during adaptation, as can be experienced in the non-static adaptor versions at http://www.mvr.mcgill.ca/Fred/research.htm#contourShapePerception.

Spatial after-effects are useful tools for exploring the color selectivity of spatial mechanisms. If an after-effect produced from adaptation and test stimuli of different color is smaller than that from adaptation and test stimuli of the same color, one can reasonably conclude that the mechanisms underlying the after-effect are selective for color direction.

What should we expect regarding the selectivity of the SFAE and SAAE to color direction? Gheorghiu and Kingdom (2006) found that both after-effects were selective for the polarity of luminance contrast, and on the basis of this finding one might expect the after-effects to be selective for color direction. Additional support for this prediction comes from studies showing that the tilt after-effect is selective to color (Broerse, Over, & Lovegrove, 1975; Elsner, 1978; Held & Shattuck, 1971; Kavadellas & Held, 1977; Lovegrove & Over, 1973; Lovegrove & Mapperson, 1981; Shattuck & Held, 1975; Smith & Over, 1976) (though perhaps surprisingly one study, that of Magnussen & Kurtenbach (1979) showed that the tilt after-effect was *not* selective to luminance polarity). Clifford, Spehar, Solomon, Martin, and Zaidi (2003) have recently shown that the related tilt illusion, in which the perceived orientation of a grating is altered by the presence of a differently oriented surround grating, is also color selective; they found that the illusion was reduced if test and surround differed in color direction. Interestingly however, Forte and Clifford (2005) found that if the color difference in the tilt illusion was along the chromatic–luminance dimension, the illusion was only reduced if monocular mechanisms were allowed to contribute, i.e., there was little-or-no reduction if binocular mechanisms contributed. This last result is important because it suggests that spatial mechanisms subserved by purely binocular neurons may not be color selective. Gheorghiu and Kingdom (2007) have shown that the SFAE and SAAE are very likely mediated by mechanisms sensitive to *local curvature*, rather than to either local orientation or global shape frequency/amplitude. Given that curvature-encoding neurons have been found predominantly in higher visual areas (Gallant, Braun, & van Essen, 1993; Gallant, Connor, Rakshit, Lewis, & van Essen, 1996; Pasupathy & Connor, 1999, 2001, 2002) where neurons are mostly binocular (Neri, 2005; Watanabe, Tanaka, Uka, & Fujita, 2002), we might therefore expect the SFAE/SAAE to be only weakly, if at all color selective along the chromatic–luminance dimension.

To test whether contour-shape encoding mechanisms are tuned to color direction, we have compared SFAEs/SAAEs for adaptor-test combinations defined along the same with along different color directions. The color directions have been defined within a modified version of the MacLeod–Boynton color space (MacLeod & Boynton, 1979). Stimuli defined along the three axes of the MacLeod–Boynton color space stimulate the 'red-green', 'blue-yellow' and 'luminance' post-receptoral mechanisms that have been isolated psychophysically (Cole, Hine, & McIlhagga, 1993; Krauskopf, Williams, & Heeley, 1982; Norlander & Koenderink, 1983; Sankeralli & Mullen, 1997; Stromeyer, Cole, & Kronauer, 1985). We chose to define the stimuli along the cardinal axes because these color directions are arguably the most likely to reveal selectivity in contour-shape encoding.

2. General methods

2.1. Observers

One of the two authors (EG) and one undergraduate volunteer (GI) participated in the study. Both subjects had normal or corrected-to-normal visual acuity.

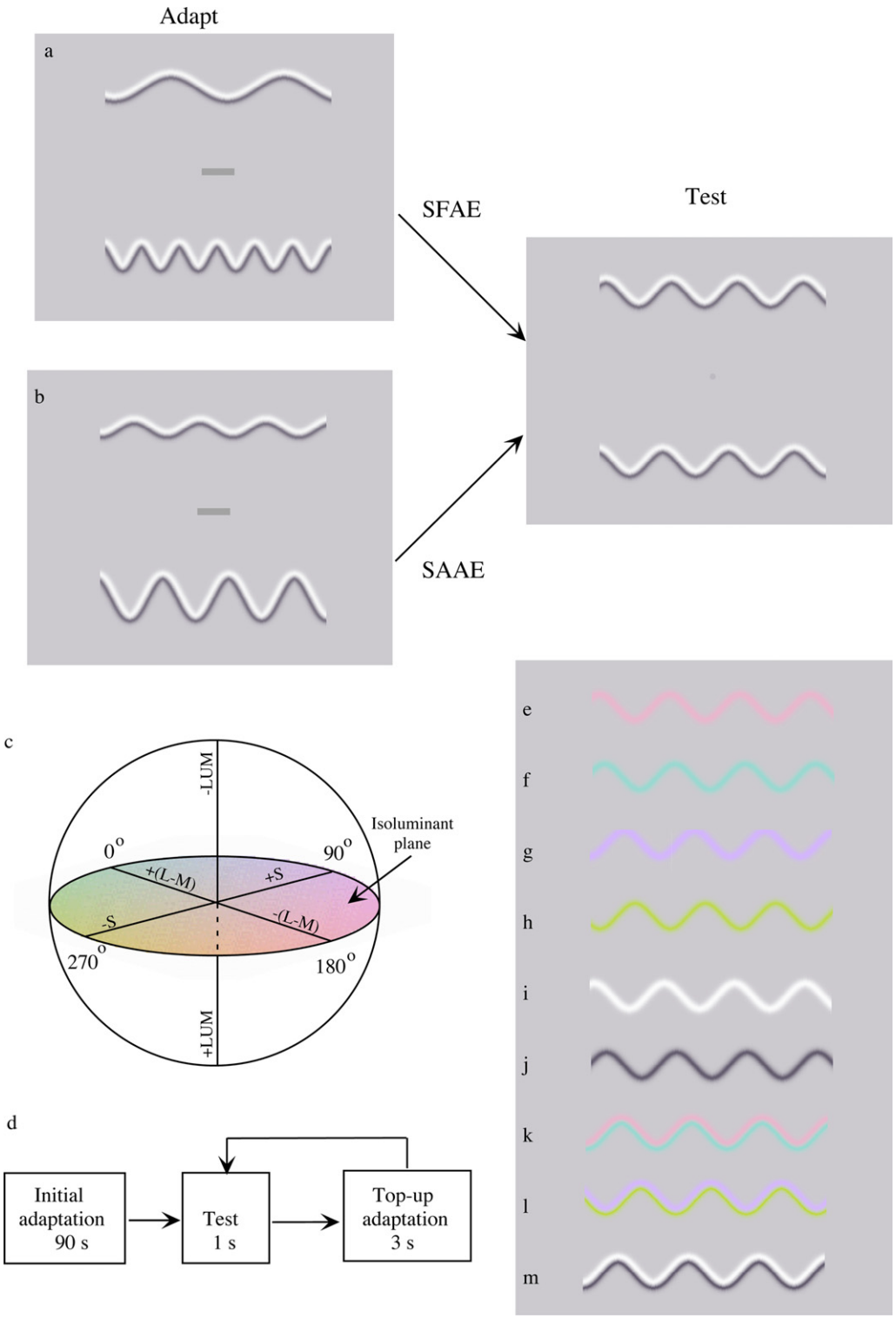

Fig. 1. Stimuli used in the experiments. One can experience (a) the shape-frequency after-effect, or SFAE and (b) the shape-amplitude after-effect, or SAAE by moving one's eyes back and forth along the markers located midway between the pair of adapting contours (left) for about 90s, and then shifting one's gaze to the middle of the test contour pair (right). (c) Modified version of the MacLeod–Boynton color space used to define color direction. (d) Schematic representation of the adapting and test procedure—see text for details. (e)–(m) example contours used in the experiments: (e) 'red'; (f) 'green'; (g) 'blue'; (h) 'yellow'; (i) 'bright'; (j) 'dark'; (k) 'red-green'; (l) 'blue-yellow', and (m) 'bright-dark'.

2.2. Stimuli—generation and display

The stimuli were generated by a VSG2/5 video-graphics card (Cambridge Research Systems) with 12-bits contrast resolution, and presented on a Sony Trinitron monitor, at 120 Hz frame rate 1024×768 spatial resolution. The R (red), G (green), and B (blue) outputs of the monitor were gamma-corrected after calibration with an Optical photometer (Cambridge Research Systems). The spectral emission functions of the R, G, and B phosphors were measured using a PR 640 spectral radiometer (Photo Research), with the monitor screen filled with red, green or blue at maximum luminance. The CIE coordinates of the phosphors were R: $x = 0.624$, $y = 0.341$; G: $x = 0.293$, $y = 0.609$; and B: $x = 0.148$, $y = 0.075$. The stimuli were presented in the centre of the monitor on a mid-gray background with CIE chromaticity $x = 0.282$ and $y = 0.311$, and mean luminance of 40 cd/m^2.

2.3. Stimuli—cardinal axes

Example stimuli are shown in Fig. 1. Adaptation and test stimuli consisted of pairs of 2D sine-wave-shaped contours that were defined along the cardinal axes of a modified version of the MacLeod–Boynton color space (MacLeod & Boynton, 1979), shown in Fig. 1c. Each axis defines how long– (L), medium– (M), and short– (S) wavelength cone contrasts are combined post-receptorally. The axes are termed LUM, L–M, and S, though sometimes these are referred to in the text by the commonly used terms 'luminance', 'red-green', and 'blue-yellow', even though these terms are inaccurate as descriptors of the hues involved. The term cardinal indicates that each stimulus uniquely stimulates one of the three post-receptoral mechanisms.

The cone contributions to the three cardinal axes are defined as follows. Cone contrast for the L cone is defined as $L_c = \Delta L/L_b$, and similarly for the M and S cones ($M_c = \Delta M/M_b$; $S_c = \Delta S/S_b$). The denominator in each term refers to the cone excitation produced by the contour's d.c., a mid-gray color with CIE chromaticity $x = 0.282$ and $y = 0.311$, and luminance of 40 cd/m^2. The nominator in each cone contrast term represents the difference in cone excitation between the peak of the contour's modulation and the d.c. The LMS cone excitations assigned to each pixel were converted to RGB phosphor intensities using the cone spectral sensitivity functions provided by Smith and Pokorny (1975) and the measured RGB spectral functions of the monitor. Current estimates of the cone contrast inputs to the three cardinal mechanisms are: $kL_C + M_C$ for the luminance mechanism, $L_C - M_C$ for the mechanism that differences L and M cone contrasts, and $S_C - (L_C + M_C)/2$ for the mechanism that differences S from the sum of L plus M cone contrasts (Cole et al., 1993; Sankeralli & Mullen, 1997; Stromeyer et al., 1985). The parameter k determines the relative weighting of the L and M cone contrast inputs to the luminance mechanism, and it varies between observers. The cone contrasts necessary to make the axes orthogonal are:

$$\mathrm{LUM} = L_C + M_C + S_C \tag{1}$$

$$L - M = L_C - kM_C + S_C(1 - k)/2 \tag{2}$$

$$S = S_C \tag{3}$$

Stimulus contrast was defined as follows: for LUM, the contrast assigned to each cone; for L–M, the difference in cone contrasts; and for S, the contrast assigned to the S cone.

2.4. Stimuli—contours

The cross-sectional profiles of the contours were of two types: even-symmetric and odd-symmetric. Even-symmetric profiles (Figs. 1d–i) were generated according to a Gaussian function:

$$I(d) = I_{\mathrm{mean}} \pm I_{\mathrm{mean}} \cdot C \cdot \exp[-(d^2)/(2\sigma^2)] \tag{4}$$

where d is the distance from the centre of the contour in a direction perpendicular to the tangent, I_{mean} is the background color/intensity, C contrast and σ the space-constant, or standard deviation, that determined the width of the contour. The $\pm$ sign determined the polarity of the contour. Odd-symmetric luminance profiles (Fig. 1j–l) were generated according to a first derivative (1D) of a Gaussian function:

$$I(d) = I_{\mathrm{mean}} \pm I_{\mathrm{mean}} \cdot C \cdot \exp(0.5) \cdot (d/\sigma) \cdot \exp[-(d^2)/(2\sigma^2)] \tag{5}$$

In this particular form of a 1D Gaussian, the term exp(0.5) gives the profile the same peak or trough value as the Gaussian function in Eq. (4). For both even-symmetric and odd-symmetric cross-sectional profiles we used a σ of 0.1 deg, which for the odd-symmetric contours resulted in a peak spatial frequency of 1.5 c/deg. Our contours were designed to have a constant cross-sectional width, and the method we used to achieve this is given in Gheorghiu and Kingdom (2006).

2.5. Procedure—isoluminant settings

Due to subject variation in the relative weightings of the L and M cone inputs to the luminance mechanism, it was necessary to ensure that the L–M stimuli were isoluminant. We also wanted to ensure that the S-cone isolating stimuli were isoluminant. To measure the isoluminant point for the L–M and S contours we used the criterion of minimum perceived motion. We used pairs of sine-wave-shaped contours arranged as described for the main experiment (see below), with an odd-symmetric profile, a shape-amplitude of 0.43 deg and a shape-frequency of 0.43 c/deg. The two contours were set to drift in opposite directions at about 1.0 Hz. The contrast of the L–M contours was set to 0.1 and the S contours to 0.5. The subjects added or subtracted equal amounts of L and M cone contrast by pressing a key on the response box until the perceived motion stopped or was minimal. Each subject made between 10 and 15 settings per session, and there were six sessions. We calculated the average added L+M cone contrast from all measurements. For the L−M defined contour, the added L+M contrast was used to estimate the ratio of L to M cone contrasts in the luminance mechanism, that is, the parameter k in Eq. (2). Parameter k was found to be 2.408 for subject EG and 1.398 for subject GI. For the S defined contour, the L+M contrast was used to calculate the ratio of luminance to color contrast required to obtain isoluminance. This was found to be 0.029 for subject EG and −0.0023 for subject GI.

2.6. Procedure—contrast matching

Contrast matching experiments were carried out to equate the perceived contrast of the L–M, LUM, and S contours. Again we used pairs of contours arranged as in the main experiment (see below). The matched contrast was determined using an ongoing, two-interval sequential presentation. One interval contained a pair of L–M (or a LUM) contours and the other a pair of S contours of fixed contrast, $S_C = 0.45$. The duration of each interval was 1 s. In order to avoid the occurrence of sharp luminance transients we presented the stimuli in a raised cosine temporal envelope of 1 s half-period. Subjects used the keys on the response box to adjust the contrast of either the L–M or LUM contours until they matched the perceived contrast of the S contour. There was no time limit for the contrast matching procedure. Each subject made 10 settings from which the mean value was estimated. This was repeated six times on different days. The mean value of L–M contrast was 0.0575 for subject EG and 0.088 for subject GI, and the mean value of LUM contrast was 0.0481 for subject EG and 0.056 for subject GI.

2.7. Procedure—measuring the SFAE and SAAE

Adapting and test stimuli consisted of pairs of 2D sinusoidal-shaped contours as shown in Fig. 1. For the SFAE, the adaptor pair consisted of contours with a shape-amplitude of 0.43 deg and shape frequencies of 0.25 and 0.75 c/deg, giving a geometric mean shape-frequency of 0.43 c/deg. For the SAAE, the shape-frequency of the adaptor pair was 0.43 c/deg, while the shape-amplitudes were 0.25 and 0.75 deg, giving a geometric mean shape-amplitude of 0.43 deg. The two adaptors and tests were presented in the center of the monitor 3 deg above and below the fixation marker.

Each session began with an initial adaptation period of 90 s, followed by a repeated test of 1 s duration interspersed with top-up adaptation periods of 3 s. A schematic representation of the adapting and test procedure is shown in Fig. 1d. During the adaptation period, the shape-phase of the contour was randomly changed every 1 s in order to prevent the formation of afterimages and to minimize the effects of local orientation adaptation. In order to minimize sharp luminance transients the contours were presented in a raised cosine temporal envelope of 1 s half-period. The presentation of each test contour was signaled by a tone. The display was viewed in a dimly lit room at a viewing distance of 100 cm. Subjects were required to fixate on the marker placed between each pair of contours for the entire session.

A staircase method was used to estimate the point of subjective equality, or PSE. For the SFAE, the geometric mean shape-frequency of the two test contours was held constant at 0.43 c/deg during the test period while the computer varied the relative shape-frequencies of the two test contours in accordance with the subject's response. At the start of the test period the ratio of the two test shape-frequencies was set to a random number between 0.33 and 3. On each trial subjects indicated via a button press whether the upper or lower test contour had the higher perceived shape-frequency. The computer then changed the ratio of shape-frequencies by a factor of 1.06 for the first five trials and 1.015 thereafter, in a direction opposite to that of the response, i.e., towards the PSE. The session was terminated after 25 trials. The shape-frequency ratio at the PSE was calculated as the geometric mean shape-frequency ratio of the two tests, with the test at the lower shape-frequency adaptor position as the nominator, averaged across the last 20 trials. Six measurements were made for each condition, three in which the upper adaptor had the higher shape-frequency (75 c/deg) and three in which the lower adaptor had the higher shape-frequency. In addition we measured for each condition the shape-frequency ratio at the PSE without adaptor. To obtain an estimate of the size of the SFAE we calculated the difference between each log with-adaptor shape-frequency ratio at the PSE and the average of the log no-adaptor shape-frequency ratio at the PSE. We then calculated the mean and standard error of these differences, and these are the values shown in the graphs.

The procedure for measuring the SAAE followed the same principle as for the SFAE. The computer varied the relative shape-amplitudes of the two tests in accordance with the subject's response, while the geometric mean shape-amplitude of the two test contours was held constant at 0.43 deg.

3. Experiment 1. Selectivity to cardinal polarity?

In this experiment we examined whether contour-shape-encoding mechanisms are selective to chromatic and luminance contrast-polarity. Contours were even-symmetric (Fig. 1e–j) and odd-symmetric (Fig. 1k–m). For each cardinal axis there were six adaptor-test conditions. For example with the L–M contours we used: (a) adaptor and test both red; (b) adaptor and test both green; (c) adaptor red and test green; (d) adaptor green and test red; (e) adaptor and test both red–green, and (f) adaptor red–green and test green–red. Corresponding adaptor-test combinations were used for contours defined along S and LUM cardinal axes. For all 18 adaptor-test combinations (3 cardinal directions × 6 adaptor-test conditions) both SFAEs and SAAE were measured.

Fig. 2 shows SFAEs and Fig. 3 SAAEs. Same adaptor-test polarities are shown as white bars and opposite adaptor-test polarities as gray bars. The results show that in almost all instances both after-effects are reduced when adapting and test contours are of opposite polarity, for both even- and odd-symmetric contours. The exceptions are the RG/GR and WD/DW conditions in subject GI's SFAE data. These are almost certainly anomalous data points that tend to arise when such a large number of conditions are tested (2 subjects × 2 after-effects × 18 conditions = 72 in total). Indeed in our previous study we found significant polarity-specificity in a similar WD/DW condition, in three naïve subjects and the two authors (the bd/db condition in Fig. 2 of Gheorghiu & Kingdom, 2006). The figure also shows that the size of the after-effects in the same-polarity conditions is similar for the chromatic and luminance contours in all subjects.

To test whether the after-effects are significantly larger for same versus opposite polarities we performed a three-way between-subjects ANOVA (analysis of variance) with combination (same polarity vs. opposite polarity), phase (even-symmetric positive vs. even-symmetric negative vs. odd-symmetric) and cardinal axis (red–green vs. blue–yellow vs. luminance) as factors, on both the SFAE and SAAE data. The main effect of Combination was significant (SFAE: $F(1,1) = 33.45$, $p < 0.01$; SAAE: $F(1,1) = 23.46$, $p < 0.01$). Phase was not significant (SFAE: $F(1,2) = 2.34$, $p = 0.113$; SAAE: $F(1,2) = 0.44$, $p = 0.647$). The effect of cardinal axis was not significant (SFAE: $F(1,2) = 0.63$, $p = 0.54$; SAAE $F(1,2) = 1.05$; $p = 0.364$). In addition, we performed a three-way ANOVA analysis to test whether the opposite polarity after-effects (gray bars) were significantly different from zero, i.e., from the non-adapted condition. They were significantly different from zero (SFAE: $F(1,1) = 11.67$, $p < 0.01$; SAAE: $F(1,1) = 41.59$; $p < 0.01$).

4. Experiment 2. Selectivity to cardinal axis?

In this experiment we examined whether contour-shape encoding mechanisms are selective for cardinal axis. We compared the after-effects using adaptor and test contours defined along the same with along different cardinal axes. The contours all had odd-symmetric profiles (Fig. 1k–m). All combinations of L–M, S and LUM, adaptors and tests were tested, for both SFAEs and SAAEs.

Fig. 4a shows SFAEs and Fig. 4b shows SAAEs. Adaptor-test combinations defined along the same cardinal axes are shown as white bars, along different chromatic cardinal axes as black bars and along chromatic versus luminance axes as gray bars. The results show (i) large SFAEs and SAAEs with adaptor and test contours defined along the same cardinal axes (white bars); (ii) reduced SFAEs and SAAEs with adaptor and test contours defined along different chromatic cardinal axes (black bars), (iii) reduced but still sizeable SFAEs and SAAEs with adaptors defined along chromatic axes and tests defined along the luminance axis (first two gray bars in each panel), except SFAE for subject GI, and (iv) a large degree of transfer between luminance-defined adaptors and chromatic-defined tests (last two gray bars). In short, the results indicate that both after-effects are selective for cardinal axis, except in the case

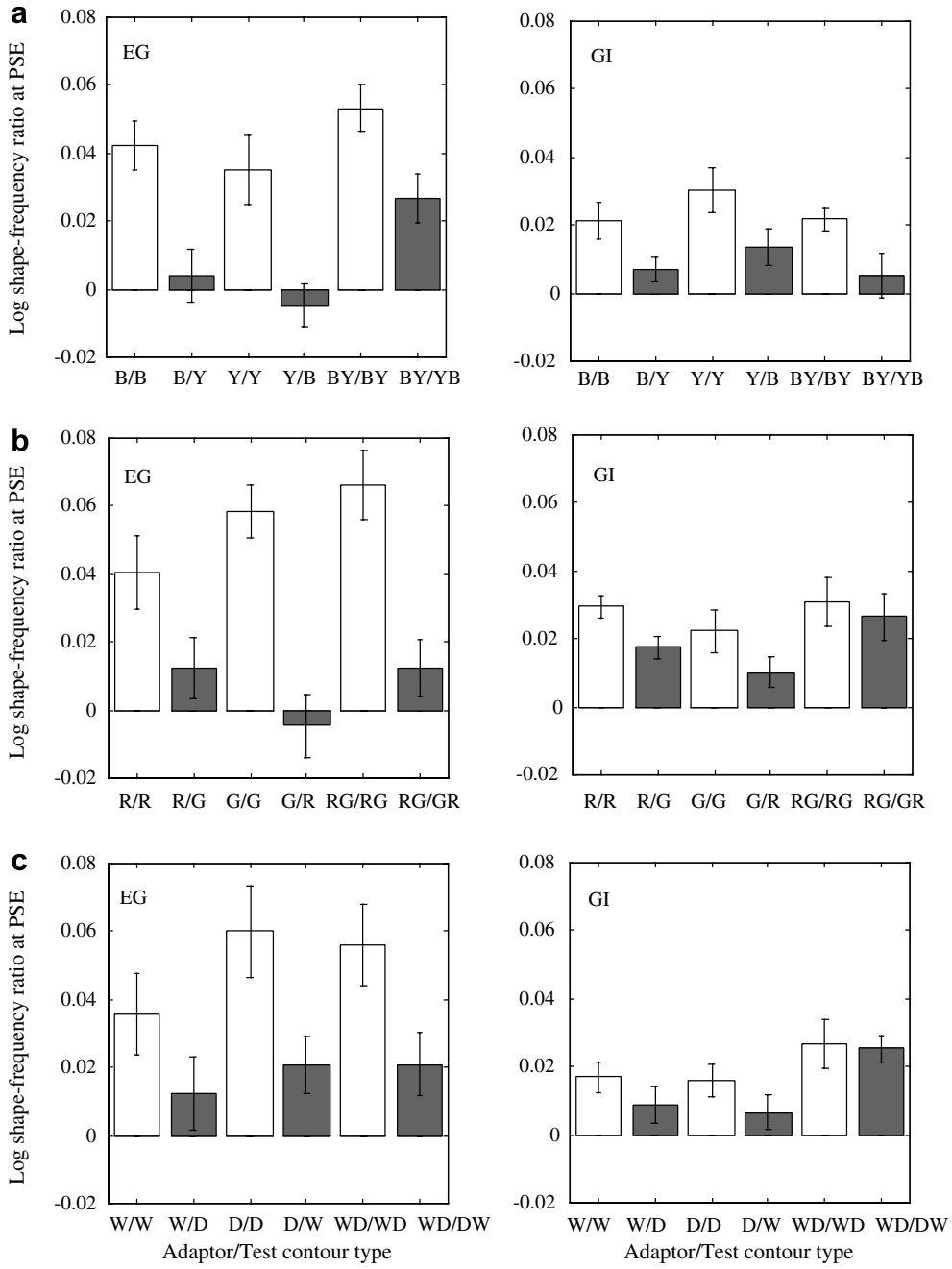

Fig. 2. SFAEs for adaptor-test combinations with the same (white bars) and opposite (gray bars) polarities for (a) blue–yellow (b) red–green and (c) luminance polarities. B, blue; Y, yellow; BY, blue–yellow; YB, yellow–blue. R, red; G, green; RG, red–green; W, bright; D, dark; WD, bright–dark.

of the SFAE when defined along the chromatic–luminance dimension.

To test whether the after-effects are overall significantly larger for same versus different cardinal axes we performed a two-way between-subjects ANOVA with factors combination (same vs. different) and cardinal axis of adaptor. For the different conditions, the two test cardinal axes for each cardinal axis of adaptor were averaged (e.g. for a red–green adaptor, both blue–yellow and luminance tests were averaged). For the SFAE the difference between the same and different combinations was not quite significant at the $p = 0.05$ level ($F(1,1) = 3.88$, $p = 0.106$). However, if we remove the luminance conditions from the data the difference is significant ($F(1,1) = 11.9$, $p < 0.05$). For the SAAE the overall difference between same and different is significant ($F(1,1) = 12.6$, $p < 0.05$). For the factor of cardinal axis of adaptor there are no significant differences for either SFAE ($F(1,5) = 0.99$, $p = 0.5$) or SAAE ($F(1,5) = 4.21$, $p = 0.07$).

In addition, we performed a two-way between-subjects ANOVA to test whether the after-effects in the different conditions were significantly different from zero. Factors were Combination (different vs. baseline) and type of combination (blue–yellow vs. red–green, bright–dark vs. red–

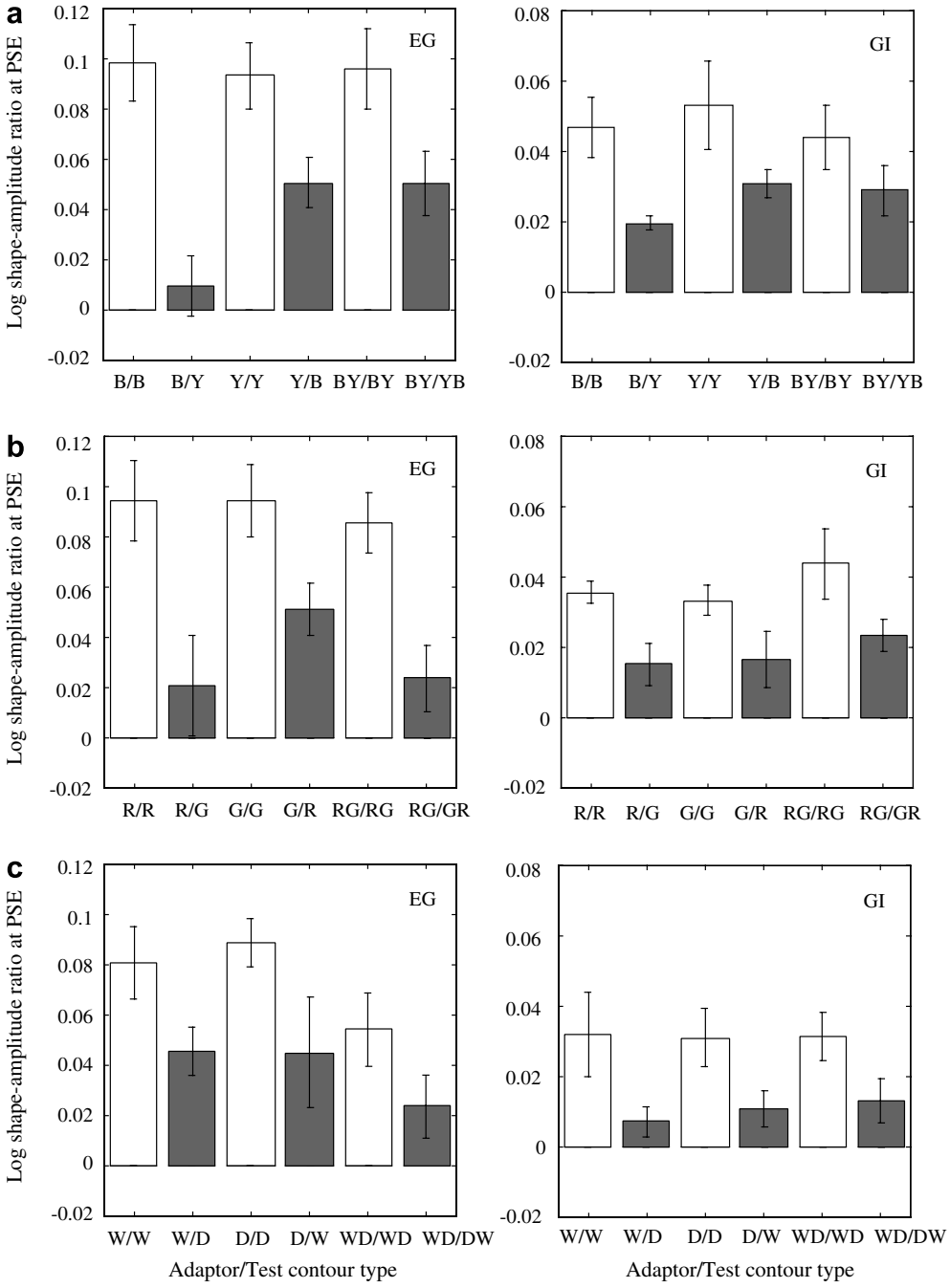

Fig. 3. SAAEs for adaptor-test combinations with the same (white bars) and opposite (gray bars) polarities. See legend of Fig. 2 for further details.

green, red–green vs. blue–yellow, etc.). The different conditions of both after-effects were found to be significantly different from zero (SFAE: $F(1,1) = 15.67$, $p < 0.01$; SAAE: $F(1,1) = 32.81$, $p < 0.01$). Type of combination was not however significant (SFAE: $F(1,11) = 0.57$, $p = 0.82$; SAAE: $F(1,1) = 0.53$, $p = 0.84$).

5. Experiment 3. Luminance artifacts?

We have found large SFAEs and SAAEs for both the L–M and S contours (Figs. 2 and 3). We went to pains to minimize the possibility that our ostensibly isoluminant contours contained luminance artifacts by (a) establishing the isoluminance point for each subject using minimum motion; (b) using Gaussian and first derivative of a Gaussian cross-sectional profiles with a relatively large space constant of 0.1 deg; (c) presenting the contours in a raised cosine temporal envelope to remove sharp temporal transients. However, even with these procedures we cannot rule out the possibility of luminance artifacts. The two likely sources of luminance artifact are (1) an isoluminant setting that is inappropriate for contour-shape processing (we used

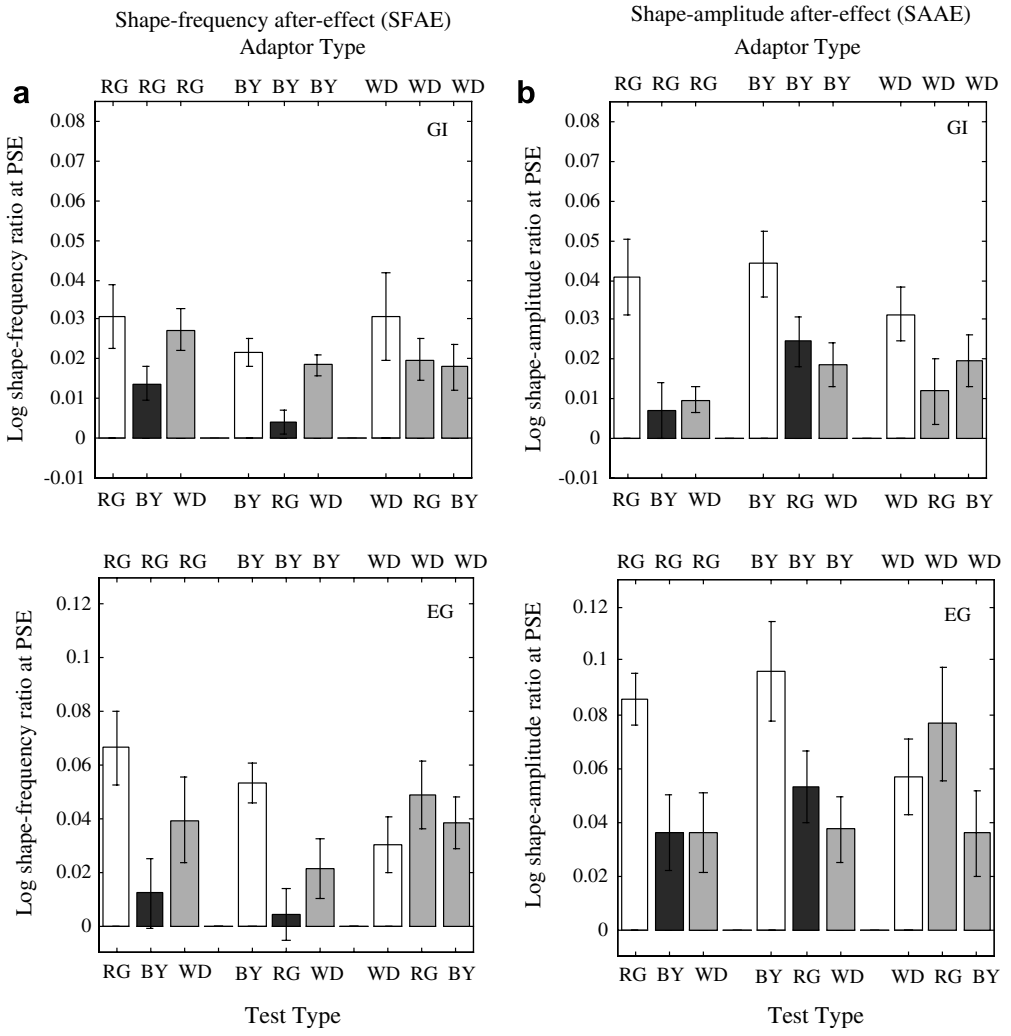

Fig. 4. (a) SFAEs and (b) SAAEs for adaptor/test combinations defined along the same cardinal axes (RG/RG, BY/BY, and WD/WD) are shown as white bars, along different chromatic cardinal axes (RG/BY and BY/RG) as black bars and along chromatic versus achromatic cardinal axes (RG/WD, BY/WD, WD/RG, and WD/BY) as gray bars.

the minimum motion method) and (2) chromatic aberration (Thibos, Bradley, Still, Zhang, & Howarth, 1990). In this section we consider each in turn.

5.1. Incorrect isoluminance setting?

If the isoluminance setting obtained using the minimum motion method (Section 2.5) was inappropriate for the mechanisms mediating the processing of contour-shape, then a residual luminance signal, similar in profile to that of the contour's cross-sectional profile but of one or other polarity, will be available to those mechanisms. If such a signal exists, it should be possible to cancel it by adding an appropriate amount and polarity of luminance contrast. We therefore measured SFAEs and SAAEs using odd-symmetric L–M and S contours, adding various amounts of luminance contrast to the adaptors, but not tests. There were eleven values of added luminance contrast: −0.2, −0.1, −0.05, −0.025, −0.0125, 0.0, 0.0125, 0.025, 0.05, 0.1, and 0.2.

Fig. 5 shows SFAEs (open symbols) and SAAEs (gray filled symbols) for subject EG as a function of added luminance contrast, for L–M (squares) and S (circles) contours. Both after-effects are obtained at all values of added luminance contrast. There is no hint of a significant drop in either after-effect at some positive or negative added luminance contrast; the only hint of a minimum is at zero added luminance contrast.

Our second method for testing whether our chromatic contours contained a matched-in-profile residual luminance signal is to compare after-effects obtained using chromatic-adaptors/luminance-tests at two luminance polarities. Given our previous finding that the after-effects are reduced when adapting and test contours are of opposite luminance polarity (Experiment 1: Figs. 2 and 3, and Gheorghiu & Kingdom, 2006), any after-effect from a chromatic adaptor that is due to a residual luminance signal

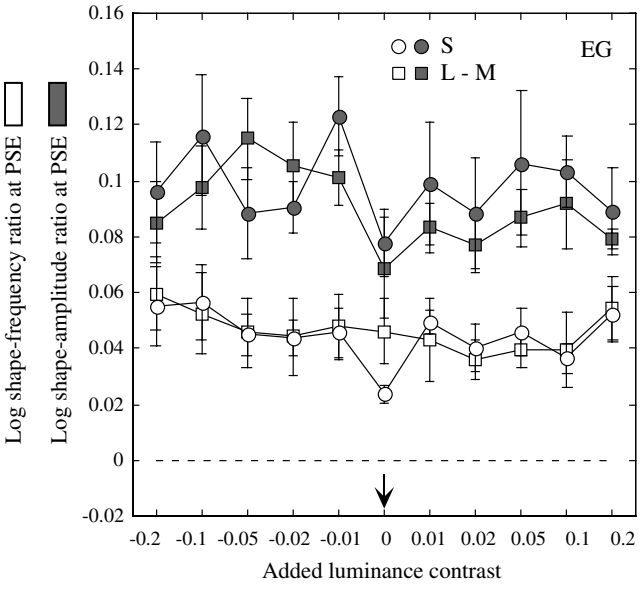

Fig. 5. SFAEs (open symbols) and SAAEs (gray filled symbols) as a function of the amount of luminance contrast added to the adapting contours for L–M (squares) and S (circles) contour-shapes.

should be polarity dependent. We used contours with odd-symmetric profiles, and tested with L–M, S and LUM adaptors. The LUM test contours were either 'bright-dark' or 'dark-bright'. We used six adaptor-test conditions: (a) adaptor 'red-green' and test 'bright-dark'; (b) adaptor 'red-green' and test 'dark-bright'; (c) adaptor 'blue-yellow' and test 'bright-dark'; (d) adaptor 'blue-yellow' and test 'dark-bright'; (e) adaptor 'bright-dark' and test 'bright-dark', and (d) adaptor 'bright-dark' and test 'dark-bright'.

Fig. 6a shows SFAEs and Fig. 6b SAAEs for all six adaptor-test combinations. First, note that with luminance adaptors/tests the after-effects are reduced when adaptor and test are of opposite luminance polarity. Second, similar sized after-effects are obtained for all chromatic-adaptor and luminance-test combinations. To test whether the after-effects obtained with chromatic adaptors and luminance tests varied significantly with the polarity of the test we performed a two-way ANOVA with test polarity (WD vs. DW) and cardinal axis (red–green vs. blue–yellow) as factors. The effect of test polarity was not significant (SFAE: $F(1,1) = 0.07$, $p = 0.83$; SAAE: $F(1,1) = 20.44$, $p = 0.14$). The effect of cardinal axis was also not significant (SFAE: $F(1,1) = 0.29$, $p = 0.68$; SAAE: $F(1,1) = 15.56$, $p = 0.158$).

The results of both these experiments are not consistent with the after-effects obtained using chromatic contours being mediated by a residual luminance signal arising from an incorrect isoluminance setting.

5.2. Chromatic aberration?

Longitudinal and transverse chromatic aberration can introduce a luminance signal into an ostensibly isoluminant stimulus (Thibos et al., 1990), with transverse chromatic aberration increasing with eccentricity (Thibos, Walsh, & Cheney, 1987). A widely adopted method to minimize the effects of chromatic aberration in chromatic stimuli is to use Gaussian-windowed stimuli with a space constant σ of at least 0.15 deg (Kingdom, Simmons, & Rainville, 1999; Mullen & Beaudot, 2002; Scharff & Geisler, 1992), as this removes spatial frequencies above about 3 c/deg (Scharff & Geisler, 1992). We have used a slightly smaller σ of 0.1 deg as we wanted to use contours with good spatial definition when sinusoidally modulated. To test whether the after-effects in our chromatic contours resulted from a luminance signal introduced by chromatic aberration we compared the after-effects for $\sigma = 0.1$ deg chromatic

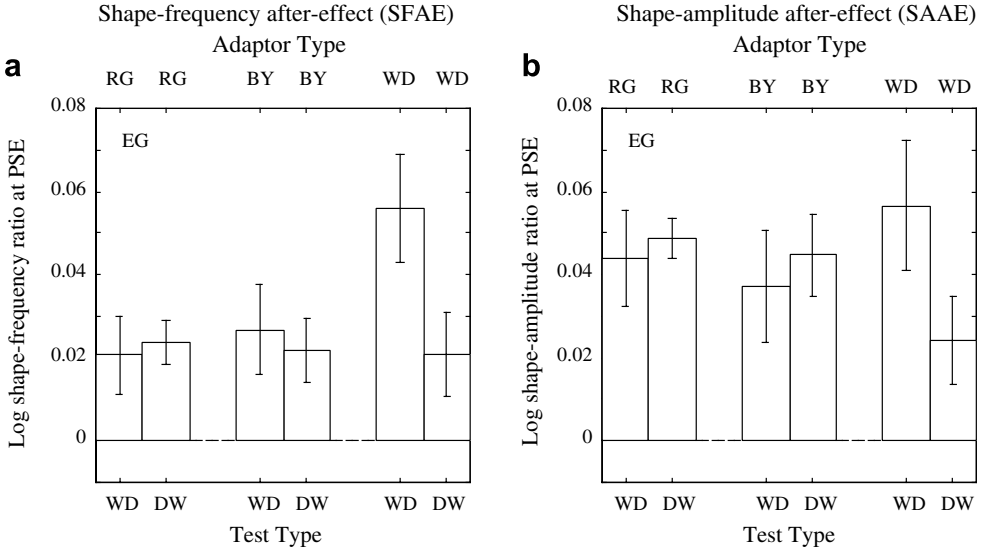

Fig. 6. (a) SFAEs and (b) SAAEs obtained using chromatic and luminance contour adaptors and luminance tests of different polarities. RG, red–green; BY, blue–yellow; WD, bright–dark; DW, dark–bright.

contour with $\sigma = 0.25$ deg chromatic contour, which is a larger σ than the minimum normally employed. We reasoned that if the after-effect was due to chromatic aberration in our $\sigma = 0.1$ deg contours, the after-effect should be eliminated in our $\sigma = 0.25$ contours. We used adaptor and test contours that were L–M, S, and LUM. If the after-effects in the chromatic $\sigma = 0.25$ conditions were eliminated, the LUM contour condition tested whether this occured because large contours per se did not produce after-effects. We also tested whether the transfer between an L–M adaptor and a LUM test was lower for the $\sigma = 0.25$ compared to $\sigma = 0.1$ deg condition. This would be expected if the transfer in the $\sigma = 0.1$ deg condition was due to chromatic aberration in the adaptor.

Fig. 7a shows SFAEs and Fig. 7b SAAEs for adaptor-test combinations with σs of 0.1 (open bars) and 0.25 deg (filled bars). Similar sized after-effects are obtained for the two σs in all cases. To test whether the after-effects were significantly different for the two values of σ we performed a two-way ANOVA with σ (0.1 vs. 0.25 deg) and cardinal axis (red–green vs. blue–yellow vs. luminance) as factors. The effect of σ was not significant (SFAE: $F(1,1) = 0.26$, $p = 0.66$; SAAE: $F(1,1) = 0.36$, $p = 0.61$). The effect of cardinal axis was also found to be not significant (SFAE: $F(1,1) = 9.89$, $p = 0.09$; SAAE: $F(1,1) = 1.63$, $p = 0.39$).

These results show that the after-effects produced by the chromatic contours do not disappear at relatively large σs, and that therefore the after-effects in our $\sigma = 0.1$ deg chromatic contours are unlikely the result of luminance artifacts introduced by chromatic aberration.

6. General discussion

The principle aim of the study was to establish whether contour-shape encoding mechanisms are tuned for color direction. Before addressing this issue however, it is worth considering the relative sizes of the SFAEs and SAAEs for our matched-in-visibility contours defined along the L–M, S, and LUM cardinal axes. Fig. 8 summarizes the results for the 'same' conditions, averaged across both even- and odd-symmetric contours, and across all experiments. As can be seen, similar sized after-effects were found for the chromatic and luminance contours. This suggests that chromaticity is an important dimension in the representation of contour-shape.

Turning now to the main issue of the study, we found that both after-effects were lower when adaptor and test differed in their within-cardinal-axis polarity (Figs. 2 and 3), and for most of the conditions also when they differed in cardinal axis. To obtain a better picture of the difference between the same and different conditions, we calculated the size of the after-effect for each different-condition as a *proportion* of the after-effect size in the corresponding same condition. One can think of this measure as the amount of transfer of the after-effect in the different condition. The results are shown in Fig. 9. For the within-axis opposite-polarity conditions (Fig. 9a), the transfer, averaged across all cardinal directions and across subjects is 0.37 for the SFAE and 0.43 for the SAAE. This finding generalizes our previous results with relatively high contrast (0.5) luminance contours (Gheorghiu & Kingdom, 2006; SFAE = 0.36), to those of lower luminance contrast (0.048 and 0.056), as well as to contours defined chromatically. For adaptor and test contours differing in cardinal axis (Fig. 9b), the amount of transfer is shown separately for the between-chromatic (BC) conditions (i.e., red–green adaptor, blue–yellow test and vice versa) and between the chromatic-and-luminance (BCL) conditions (i.e., red–green or blue–yellow adaptor, luminance test and vice versa). In order to test whether the transfer in the between-chromatic

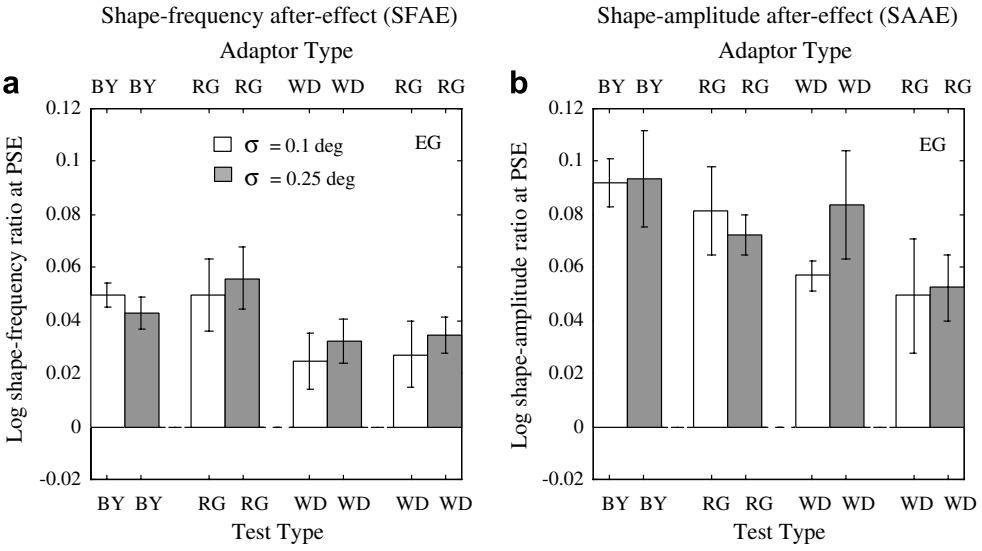

Fig. 7. (a) SFAEs and (b) SAAEs obtained using odd-symmetric contours of two different widths: $\sigma = 0.1$ deg (open bars) and $\sigma = 0.25$ deg (filled bars). RG, red–green; BY, blue–yellow; WD, bright–dark. Note that adaptors and tests are the same except for the last two bars in each figure where the adaptors are RG and the tests WD.

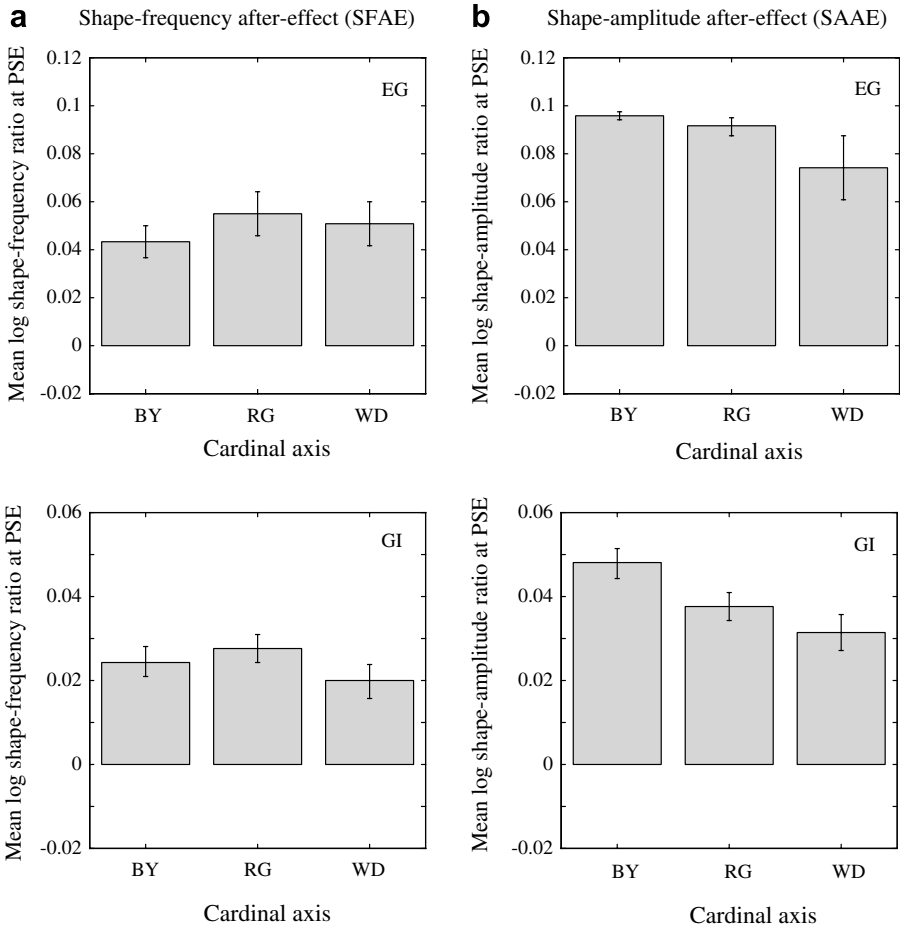

Fig. 8. Mean size of (a) SFAEs and (b) SAAEs for contours defined along the S, L–M, and LUM cardinal axes, averaged across both even- and odd-symmetric contours, and across all experiments. Separate figures for the two subjects are shown.

and between-chromatic-and-luminance conditions was significantly different for the two types of after-effect we performed a two-way ANOVA with type of after-effect (SFAE vs. SAAE) and type of transfer (BC vs. BCL) as factors. The effect of Type of after-effect was not significant ($F(1,1) = 0.17$; $p = 0.69$), whereas effect of Type of transfer was significant ($F(1,1,) = 10.89$; $p < 0.01$). The interaction between the two factors was also significant ($F(1,1) = 6.97$; $p < 0.05$).

The notable findings here are that the pattern of results in Fig. 9b differs for the SFAE and SAAE and that in the SFAE-BCL condition the transfer is large at about 0.8 in both subjects. Taken together these results imply that while contour-shape encoding mechanisms are selective for chromatic direction, it is equivocal as to whether they are selective along the chromatic–luminance dimension. We have shown previously that the SFAE and SAAE are separable curvature after-effects, suggesting that the cord and sag of a curve are coded separately (Gheorghiu & Kingdom, 2007). Why should the sag be selective along the color-luminance dimension but the cord non-selective? We do not have a good answer, but one possibility is that the cord is processed only by binocular mechanisms, while the sag is processed by both monocular and binocular mechanisms. This follows Forte and Clifford's (2005) finding that when the tilt illusion was mediated only by binocular neurons, there was almost no selectivity along the chromatic–luminance dimension. We are planning experiments to test this idea.

Although we have demonstrated selectivity of the SFAE/SAAE to the cardinal axes, we are not claiming there is anything special about the cardinal axes for contour-shape processing. Indeed, given the results of Clifford et al. (2003), who found that the tilt illusion was just as selective to color directions other than those defined as cardinal, we assume this to be the case also for the SFAE and SAAE.

6.1. Significance for the relationship between color and form

The importance of chromatic contrast (in this section 'color') in the analysis of form remains controversial (see Gegenfurtner & Kiper, 2003 for a recent review). One influential view is that color is processed separately from other attributes such as form, depth and motion (DeYoe & Van Essen, 1985; Livingstone & Hubel, 1987; Shipp & Zeki, 2002; Zeki, 1978). A corollary to this view is that color is

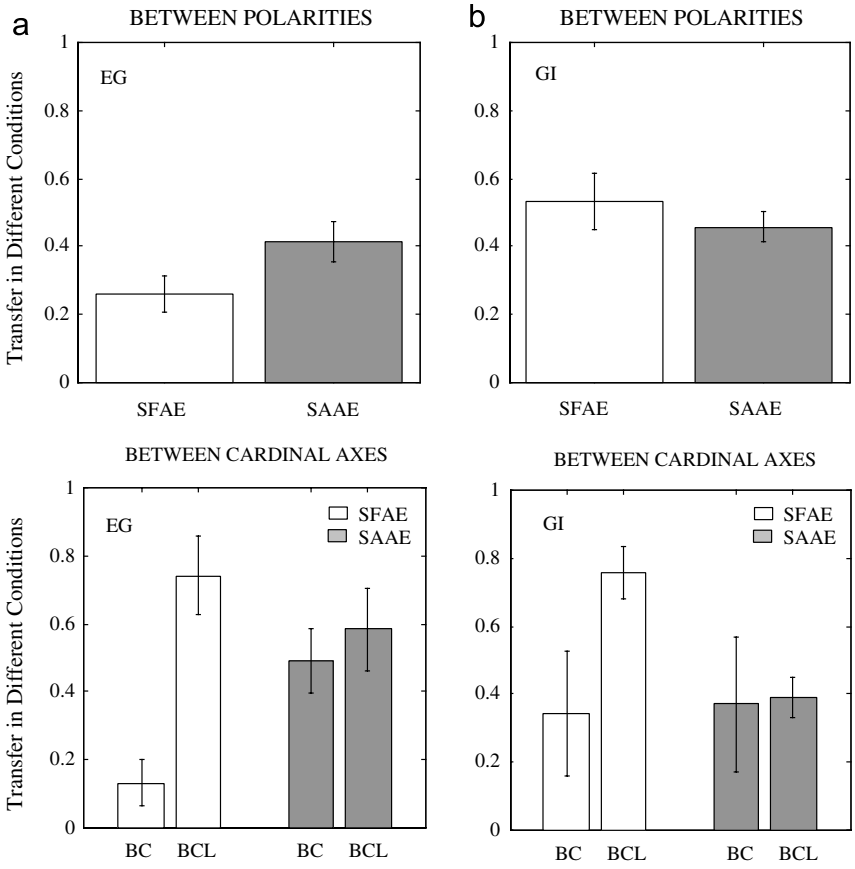

Fig. 9. The amount of transfer of the after-effects in the conditions where adaptors and tests were of a different color direction, calculated as a proportion of the size of the after-effect when adaptors and tests were of the same color direction. (a) Transfer between within-axis polarities, averaged across all cardinal directions. (b) Transfer between cardinal axis. BC = transfer between chromatic (i.e., red–green adaptor, blue–yellow test and vice versa); BCL = transfer between chromatic and luminance (i.e., red–green or blue–yellow adaptor, luminance test and vice versa). SFAEs = white bars; SAAEs = gray bars. Separate figures for the two subjects are shown.

mainly used to 'fill in the gaps' after luminance-sensitive mechanisms have provided a more-or-less complete structural description of the image (Livingstone & Hubel, 1987). Although this view accepts that color vision can provide rudimentary information about the position and shape of objects, it contends that stereopsis ('3-D' vision), motion analysis and any process that 'links-up' information distributed across space, such as to form contours, is 'color-blind'.

The psychophysical evidence for this view rests primarily on the apparent losses of perceptual abilities such as motion and stereopsis at isoluminance (Livingstone & Hubel, 1987). However, many studies of form perception employing isoluminant stimuli have shown that visual tasks once thought to be color-blind are color-sensitive, for example stereopsis (reviewed by Kingdom & Simmons, 2000; see also Simmons & Kingdom, 2002), contour detection in noise (Kingdom, Moulden, & Collyer, 1992; McIlhagga & Mullen, 1996; Mullen, Beaudot, & McIlhagga, 2000) and texture processing (Li & Lennie, 1997; McIlhagga, Hine, Cole, & Snyder, 1990; Mollon, 1989; Pearson & Kingdom, 2002). Moreover, in mixed color-and-luminance displays color has been shown to have a powerful effect on perceived shape-from-shading (Kingdom, 2003).

An important caveat to the view that color supports form perception however is that isoluminant stimuli typically require more contrast (relative to detection threshold) than isochromatic stimuli to produce the same level of performance (examples are orientation discrimination (Webster, De Valois, & Switkes, 1990), stereo-detection (Kingdom & Simmons, 2000) and radial-frequency shape detection (Mullen & Beaudot, 2002). Detection/discrimination form tasks are limited by internal noise, and the lower contrast sensitivity of form tasks at isoluminance likely reflects the higher level of internal noise in the chromatic form signal. What is interesting about the findings here is that using a task that is presumably not limited by internal noise and that taps directly the mechanisms that represent the stimulus dimension of interest, in this case curvature, we have found that color contrast is as effective as luminance contrast, even when matched for visibility. Our results are therefore arguably more in accord with those studies showing that color and orientation are conjointly represented, as evidenced by the McCollough after-effect (Houck & Hoffman, 1986; McCollough, 1965) and the studies of the tilt after-effect described in Section 1.

6.2. Relationship to neurophysiology

The neurophysiological evidence relating to the relationship between color and form processing is also controversial. Brain imaging studies have revealed a specialized color area in humans near the fusiform gyrus (Hadjikhani, Liu, Dale, Cavanagh, & Tootell, 1998; Komatsu, Ideura, Kaji, & Yamane, 1992; Zeki et al., 1991), termed by some V8 (Tootell, Hadjikhani, Liu, Cavanagh, & Dale, 1998), a finding supported by studies of cerebral a chromatopsis who show a selective loss of the sensation of hue from localized brain damage (Meadows, 1974; Zeki, 1990). However, the putative color-specialized brain area may be mainly involved in color appearance and its existence should not be considered as evidence against form-from-color processing. In most early cortical areas at least some, if not most neurons are tuned to both color and luminance contrast (Derrington, Krauskopf, & Lennie, 1984; Horowitz, Chichlinsky, & Albright, 2005; Johnson, Hawken, & Shapley, 2001; Lennie, Krauskopf, & Sclar, 1990; Thorell, De Valois, & Albrecht, 1984), and since the importance of luminance contrast for form processing is not in dispute, the existence of these color-and-luminance-sensitive neurons is supportive of a role for color in form processing. More direct neurophysiological evidence for form-from-color processing is Ts'o, Roe, & Gilbert's (2001) finding that many V2 neurons are tuned for combinations of dimensions such as color, form and disparity, and that these combinations are organized into functionally distinct columns.

The human homologs of monkey areas V4 and/or IT (inferior temporal cortex) are probably the most likely sites of the after-effects reported here. Neurophysiological studies have shown that V4 (Gallant et al., 1993; Gallant et al., 1996; Pasupathy & Connor, 1999, 2001, 2002; Schiller, 1995) and IT (Desimone, Schein, Moran, & Ungerleider, 1985) neurons are involved in coding curves, angles, and shapes. V4 neurons are color-selective (Desimone & Schein, 1987; Schein, Marrocco, & de Monasterio, 1982; Zeki, 1983) and receive inputs from color-opponent neurons (Schein & Desimone, 1990), though they are no more color selective than neurons in other visual areas (Desimone et al., 1985; Schein et al., 1982; Tanaka, Weber, & Creutzfeldt, 1986). Inferior temporal (IT) cortex neurons involved in encoding shape are also selective to color and preserve information about luminance contrast-polarity (Ito, Fujita, Tamura, & Tanaka, 1994).

Finally in the Introduction we made the distinction between feature-rich and feature-agnostic models of early visual coding. In line with our previous findings (Gheorghiu & Kingdom, 2006) the results of the present study suggest that curvature coding is feature-rich.

Acknowledgments

This research was supported by a Natural Sciences and Engineering Research Council of Canada (NSERC) Grant # OGP01217130 and Canadian Institute of Health Research (CIHR) # MOP-11554 Grant given to F.K.

References

Broerse, J., Over, R., & Lovegrove, W. J. (1975). Loss of wavelength selectivity in contour masking and after-effect following dichoptic adaptation. *Perception & Psychophysics, 17*, 333–336.

Clifford, C. W., Spehar, B., Solomon, S. G., Martin, P. R., & Zaidi, Q. (2003). Interactions between color and luminance in the perception of orientation. *Journal of Vision, 3*, 106–115.

Cole, G. R., Hine, T., & McIlhagga, W. (1993). Detection mechanisms in L-, M-, and S-cone contrast space. *Journal of the Optical Society of America A, 10*, 38–51.

Derrington, A. M., Krauskopf, J., & Lennie, P. (1984). Chromatic mechanisms in lateral geniculate nucleus of macaque. *Journal of Physiology, 357*, 241–265.

Desimone, R., Schein, S. J., Moran, J., & Ungerleider, L. G. (1985). Contour, color and shape analysis beyond the striate cortex. *Vision Research, 25*(3), 441–452.

Desimone, R., & Schein, S. J. (1987). Visual properties of neurons in area V4 of the macaque: Sensitivity to stimulus form. *Journal of Neurophysiology, 57*(3), 835–868.

DeYoe, A., & Van Essen, D. C. (1985). Segregation of efferent connections and receptive field properties in visual area V2 of the macaque. *Nature, 317*, 58–61.

Elsner, A. (1978). Hue difference contours can be used in processing orientation information. *Perception & Psychophysics, 25*, 451–456.

Forte, J. D., & Clifford, C. W. G. (2005). Inter-ocular transfer of the tilt illusion shows that monocular orientation mechanisms are color selective. *Vision Research, 45*, 2715–2721.

Gallant, J. L., Braun, J., & van Essen, D. C. (1993). Selectivity for polar, hyperbolic and Cartesian gratings in macaque visual cortex. *Science, 259*(5091), 1100–1103.

Gallant, J. L., Connor, C. E., Rakshit, S., Lewis, J. W., & van Essen, D. C. (1996). Neural responses to polar, hyperbolic and Cartesian gratings in area V4 of the macaque monkey. *Journal of Neurophysiology, 76*(4), 2718–2839.

Gegenfurtner, K. R., & Kiper, D. C. (2003). Color Vision. *Annual Review Neuroscience, 26*, 181–206.

Gheorghiu, E., & Kingdom, F. A. A. (2006). Luminance-contrast properties of contour-shape processing revealed through the shape-frequency after-effect. *Vision Research, 46*(21), 3603–3615.

Gheorghiu, E., & Kingdom, F. A. A. (2007). The spatial feature underlying the shape-frequency and shape-amplitude after-effects. *Vision Research, 47*(6), 834–844.

Hadjikhani, N., Liu, a. K., Dale, A. m., Cavanagh, P., & Tootell, R. B. (1998). Retinotopy and color sensitivity in human visual cortical area V8. *Nature Neuroscience, 1*, 235–241.

Held, R., & Shattuck, S. R. (1971). Color- and edge-sensitive channels in human visual system: Tuning for orientation. *Science, 174*(6), 314–316.

Hesse, G. S., & Georgeson, M. A. (2005). Edges and bars: Where do people see features in 1D images? *Vision Research, 45*(4), 507–525.

Horowitz, G. D., Chichlinsky, E. J., & Albright, T. D. (2005). Blue–yellow signals are enhanced by spatiotemporal luminance contrast in macaque V1. *Journal of Neuroscience, 93*, 2263–2278.

Houck, M. R., & Hoffman, J. E. (1986). Conjunction of color and form without attention: Evidence from an orientation-contingent color aftereffect. *Journal of Experimental Psychology: Human Perception and Performance, 12*(2), 186–199.

Ito, M., Fujita, I., Tamura, H., & Tanaka, K. (1994). Processing of contrast polarity of visual images in inferotemporal cortex of the macaque monkey. *Cerebral Cortex, 4*(5), 499–508.

Johnson, E. N., Hawken, M. J., & Shapley, R. (2001). The spatial transformation of color signals in the primary visual cortex of the macaque monkey. *Nature Neuroscience, 4*, 409–416.

Kavadellas, A., & Held, R. (1977). Monocularity of colour-contingent tilt after-effects. *Perception & Psychophysics, 21*, 12–14.

Kingdom, F. A. A. (2003). Color brings relief to human vision. *Nature Neuroscience, 6*, 641–644.

Kingdom, F. A. A., Moulden, B., & Collyer, S. (1992). A comparison between color and luminance contrast in a spatial linking task. *Vision Research, 32*, 709–717.

Kingdom, F. A. A., & Prins, N. (2005a). Different mechanisms encode the shapes of contours and contour-textures. *Journal of Vision, 5*(8), 463 (abstract).

Kingdom F. A. A., & Prins N. (2005b). Separate after-effects for the shapes of contours and textures made from contours. *Perception, 34*(suppl.), 92 (abstract).

Kingdom, F. A. A., Simmons, D. R., & Rainville, S. (1999). On the apparent collapse in stereopsis in random-dot-stereograms at isoluminance. *Vision Research, 39*, 2127–2141.

Kingdom, F. A. A., & Simmons, D. R. (2000). The relationship between color vision and stereoscopic depth perception (invited paper). *Journal of the Society for 3D Broadcasting and Imaging, 1*, 10–19.

Komatsu, H., Ideura, Y., Kaji, S., & Yamane, S. (1992). Color selectivity of neurons in the inferior temporal cortex of the awake macaque monkey. *Journal of Neuroscience, 12*, 408–424.

Krauskopf, J., Williams, D. R., & Heeley, D. W. (1982). Cardinal directions of colour space. *Vision Research, 22*(9), 1123–1131.

Lennie, P., Krauskopf, J., & Sclar, G. (1990). Chromatic mechanisms in striate cortex of macaque. *Journal of Neuroscience, 10*(2), 649–669.

Li, A., & Lennie, P. (1997). Mechanisms underlying segmentation of colored textures. *Vision Research, 37*, 83–97.

Livingstone, M. S., & Hubel, D. H. (1987). Psychophysical evidence for separate channels for the perception of form, color, movement and depth. *The Journal of Neuroscience, 7*, 3416–3466.

Lovegrove, W. J., & Over, R. (1973). Color selectivity in orientation masking and after-effect. *Vision Research, 13*(5), 895–902.

Lovegrove, W., & Mapperson, B. (1981). Colour selectivity in the tilt after-effect: Comments upon Wade and Wenderoth. *Vision Research, 21*(3), 355–359.

MacLeod, D. I. A., & Boynton, R. M. (1979). Chromaticity diagram showing cone excitation stimuli by stimuli of equal luminance. *Journal of the Optical Society of America, 69*, 1183–1186.

Magnussen, S., & Kurtenbach, W. (1979). A test for contrast-polarity selectivity in the tilt aftereffect. *Perception, 8*(5), 523–528.

Marr, D. (1982). *Vision: A computational investigation into the human representation and processing of visual information*. San Francisco: W.H. Freeman.

Marr, D., & Hildreth, E. (1980). Theory of edge detection. *Proceedings of the Royal Society of London B, 207*, 187–217.

McCollough, C. (1965). Color adaptation of edge-detectors in the human visual system. *Science, 149*, 1115–1116.

McIlhagga, W., Hine, T., Cole, G. R., & Snyder, A. W. (1990). Texture segregation with luminance and chromatic contrast. *Vision Research, 30*, 489–495.

McIlhagga, W. H., & Mullen, K. T. (1996). Contour integration with color and luminance contrast. *Vision Research, 36*, 1265–12579.

Meadows, J. C. (1974). Disturbed perception of colors associated with localized brain lesions. *Brain, 97*, 615–632.

Mollon, J. D. (1989). 'Tho' she kneel'd in that place where they grew. The uses and origins of primate color vision. *Journal of Experimental Biology, 146*, 21–38.

Moronne, M. C., & Burr, D. C. (1988). Feature detection in human vision: A phase-dependent energy model. *Proceedings of the Royal Society of London B, 235*, 221–245.

Mullen, K. T., & Beaudot, W. H. (2002). Comparison of color and luminance vision on a global shape discrimination task. *Vision Research, 42*(5), 565–575.

Mullen, K. T., Beaudot, W. H., & McIlhagga, W. H. (2000). Contour integration in color vision: A common process for the blue–yellow, red–green and luminance mechanisms? *Vision Research, 40*, 639–655.

Neri, P. (2005). A stereoscopic look at visual cortex. *Journal of Neurophysiology, 93*(4), 1823–1826.

Norlander, C., & Koenderink, J. J. (1983). Spatial and temporal discrimination ellipsoids in color space. *Journal of the Optical Society of America, 73*, 1533–1543.

Pasupathy, A., & Connor, C. E. (1999). Responses to contour features in macaque area V4. *Journal of Neurophysiology, 82*(5), 2490–2502.

Pasupathy, A., & Connor, C. E. (2001). Shape representation in area V4: Position-specific tuning for boundary conformation. *Journal of Neurophysiology, 86*(5), 2505–2519.

Pasupathy, A., & Connor, C. E. (2002). Population coding of shape in area V4. *Nature Neuroscience, 5*(12), 1332–1338.

Pearson, P. M., & Kingdom, F. A. A. (2002). Texture-orientation mechanisms pool color and luminance. *Vision Research, 42*, 1547–1558.

Sankeralli, M. J., & Mullen, K. T. (1997). Post-receptoral chromatic detection mechanisms revealed by noise masking in three-dimensional cone contrast space. *Journal of the Optical Society of America A, 14*, 906–915.

Scharff, L. V., & Geisler, W. S. (1992). Stereopsis at isoluminance in the absence of chromatic aberration. *Journal of the Optical Society of America A, 9*, 868–876.

Schein, S. J., Marrocco, R. T., & de Monasterio, F. M. (1982). Is there a high concentration of color-selective cells in area V4 of monkey visual cortex? *Journal of Neurophysiology, 47*(2), 193–213.

Schein, S. J., & Desimone, R. (1990). Spectral properties of V4 neurons in the macaque. *Journal of Neuroscience, 10*(10), 3369–3389.

Schiller, P. H. (1995). Effects of lesions in visual cortical area V4 on the recognition of transformed objects. *Nature, 376*(6538), 342.

Shattuck, S., & Held, R. (1975). Color and edge sensitive channels converge on stereo-depth analyzers. *Vision Research, 15*(2), 309–311.

Shipp, S., & Zeki, S. (2002). The functional organization of area V2, 1: Specialization across stripes and layers. *Visual Neuroscience, 19*, 187–210.

Simmons, D. R., & Kingdom, F. A. A. (2002). Interactions between chromatic- and luminance-contrast-sensitive stereopsis mechanisms. *Vision Research, 42*, 1535–1545.

Smith, A. J., & Over, R. (1976). Color-selective tilt after-effects with subjective contours. *Perception & Psychophysics, 20*, 305–308.

Smith, V. C., & Pokorny, J. (1975). Spectral sensitivity of the foveal cone photopigments between 400 and 700 nm. *Vision Research, 15*, 161–171.

Stromeyer, C. F., III, Cole, G. R., & Kronauer, R. E. (1985). Second-site adaptation in the red–green chromatic pathways. *Vision Research, 25*(2), 219–237.

Tanaka, M., Weber, H., & Creutzfeldt, O. D. (1986). Visual properties and spatial distribution of neurons in the visual association area on the prelunate gyrus of the awake monkey. *Experimental Brain Research, 65*, 11–37.

Thibos, L. N., Bradley, A., Still, D. L., Zhang, X., & Howarth, P. A. (1990). Theory and measurement of ocular chromatic aberration. *Vision Research, 30*(1), 33–49.

Thibos, L. N., Walsh, D. J., & Cheney, F. E. (1987). Vision beyond the resolution limit: Aliasing in the periphery. *Vision Research, 27*(12), 2193–2197.

Thorell, L. G., De Valois, R. L., & Albrecht, D. G. (1984). Spatial mapping of monkey V1 cells with pure color and luminance stimuli. *Vision Research, 24*(7), 751–769.

Tootell, R., Hadjikhani, N., Liu, A., Cavanagh, P., & Dale, A. (1998). Color and retinotopy in human visual cortical area v8. *Investigative Ophthalmological Visual Science, 39*(4), 1129.

Ts'o, D. Y., Roe, A. W., & Gilbert, C. D. (2001). A hierarchy of the functional architecture for color, form and disparity in primate visual area V2. *Vision Research, 41*, 1333–1349.

Watanabe, M., Tanaka, H., Uka, T., & Fujita, I. (2002). Disparity-selective neurons in area V4 of macaque monkeys. *Journal of Neurophysiology, 87*(4), 1960–1973.

Watt, R. J. (1988). *Visual processing*. Hove and London: L Erlbaum Associates.

Watt, R. J., & Morgan, M. J. (1985). Spatial filters and the localization of luminance changes in human vision. *Vision Research, 24*(10), 1387–1397.

Webster, M. A., De Valois, K. K., & Switkes, E. (1990). Orientation and spatial-frequency discrimination for luminance and chromatic gratings. *Journal of the Optical Society of America A, 7*, 1034–1049.

Zeki, S. (1978). Functional specialization in the visual cortex of the rhesus monkey. *Nature, 274*, 423–428.

Zeki, S. (1983). The distribution of wavelength and orientation selective cells in different areas of monkey visual cortex. *Proceedings of the Royal Society of London. Series B Biological Sciences, 217*, 449–470.

Zeki, S. (1990). A century of cerebral achromatopsia. *Brain, 113*, 1721–1777.

Zeki, S., Watson, J. D., Lueck, C. J., Friston, K. J., Kennard, C., & Frackowiak, R. S. (1991). A direct demonstration of functional specialization in human visual cortex. *Journal of Neuroscience, 11*, 641–649.